COMPDYN 2013
4th ECCOMAS Thematic Conference on
Computational Methods in Structural Dynamics and Earthquake Engineering
M. Papadrakakis, N.D.Lagaros, V. Plevris (eds.)
Kos Island, Greece, 12–14 June 2013

FINITE ELEMENT MODELING OF "ROCKING WALLS"

Andrea Belleri[1], **Mauro Torquati**[1], **and Paolo Riva**[1]

[1] Department of Engineering, University of Bergamo
Viale Marconi 5, 24044 Dalmine – Bergamo, Italy
e-mail: andrea.belleri@unibg.it; mauro.torquati@unibg.it; paolo.riva@unibg.it

Keywords: Rocking Walls; Nonlinear Static Analyses; Nonlinear Time History Analyses; Rayleigh Damping; Acceleration Spikes.

Abstract. *Rocking walls represent an emerging solution for lateral force resisting systems in low to medium seismicity sites. The main features of these systems are the self-centering capacity after a seismic event provided by unbonded post-tensioned tendons connecting the top of the wall to the foundation and the low damage, compared to traditional reinforced concrete shear walls, being the rocking wall placed on top of the foundation with no longitudinal reinforcing bar crossing the wall-foundation joint, thus avoiding tension in concrete. These systems accommodate displacement seismic demand by the development of a concentrated gap opening between the wall and the foundation instead of an extended plastic hinge as in traditional shear walls.*

The aim of the present paper is the comparison of different rocking wall finite element modeling techniques, by means of nonlinear static and dynamic analyses, in order to highlight the influence of the system damping choice on the numerical response and the differences in terms of lateral and vertical wall displacements, base shear, neutral axis variation and compressive strain at the wall toe. The finite element models considered herein are based on nonlinear brick and plane-stress plate elements, fiber beam elements, compression only springs and concentrated rotational springs.

1 INTRODUCTION

Precast concrete structures have been successfully adopted worldwide as lateral force resisting systems of buildings in low to high seismicity areas. In the case of one to two story industrial and commercial buildings, in low to moderate seismicity areas, the structural layout is typically a hinged frame and the lateral force resistance is provided by cantilever columns connected at the base to isolated footings through mechanical connectors, pocket foundations or grouted sleeve solutions [1-3].

For higher buildings and higher seismicity levels the lateral force resistance is provided by precast concrete structures emulating cast in place reinforced concrete [4] or by jointed ductile precast concrete connections which, by means of prestressed or post-tensioned elements, eliminate or reduce the residual structural displacement and rotations after a seismic event and provide energy dissipation by means of specific details [5].

As an alternative to traditional reinforced concrete walls as lateral force resisting system, a possible precast solution, suitable for medium rise buildings in low seismicity areas, consists of precast wall panels placed on top of the foundation without providing continuity to longitudinal rebars at the foundation-wall interface; the overturning moment capacity and self-centering capability is provided by gravity loads supplemented with unbonded post-tensioned tendons. This solution is referred to as "rocking wall" and is an extension of the hybrid coupled wall system developed under the PRESSS program [5]. In this system the wall horizontal displacement demand is accommodated by the development of a single gap opening at the wall-foundation interface with no concrete in tension compared to extended cracking in the plastic hinge region at the wall base in traditional reinforced concrete walls.

During a seismic event the wall rocks at its toes, providing appropriate compressive concrete resistance in the toe region by confinement and appropriate self-centering capacity by unbonded post-tensioned tendons, exhibiting a nonlinear elastic response with a distinct stiffness reduction associated to uplift of the wall base. Due to the lack of energy dissipation, limited to the hysteresis in the concrete at the compressed toes, rocking wall systems are suitable only for low seismicity areas. For higher seismic demand additional energy dissipators, hysteretic or viscous devices among others, could be added to the wall panels leading to the so called "hybrid wall" solutions.

Experimental research was conducted on single rocking and hybrid wall panels under both quasi-static [6-8] and dynamic loading [9] proving the good performance of these systems if detailed appropriately. The dynamic interaction between rocking and hybrid walls and the rest of the structure was investigated during the DSDM project [10] in which shake table tests were conducted on a three story half-scale precast concrete structure whose lateral force resisting system consisted entirely on rocking and hybrid walls [11, 12].

Although extensive experimental tests were carried out on rocking and hybrid walls, limited information is available, to the authors' knowledge, on how to numerically model these structures [13-15] in order to capture the typical nonlinear response associated to wall base uplift. The present paper focuses on numerical modeling of rocking walls investigating the effects of different modeling techniques in both nonlinear static and dynamic analyses. The rocking wall chosen as reference for the present study is extrapolated from the aforementioned DSDM project [11, 12]. Being the aim of the paper the investigation of finite modeling techniques, there is no interest in modeling the whole building in order to capture rocking wall and floors interaction and wall foundation influence; therefore the floors are modeled as point masses and the foundation is deliberately made rigid.

The finite element models considered herein are based on three dimensions (3D), two dimensions (2D) and one dimension (1D) elements, being the 3D and 2D nonlinear brick and

plane-stress plate elements, respectively, and the 1D fiber beam elements, compression only springs and concentrated rotational spring at the base of the wall. The comparison between the investigated modeling techniques is carried out both in global terms, as base shear, lateral displacement and vertical uplift, and in local terms, as neutral axis variation and compressive strain at the wall toe when available. The influence of the system damping choice on the numerical response is also investigated.

2 SELECTED CASE STUDY

The selected case study considers the rocking wall adopted as lateral force resisting system for a three story half-scale precast concrete structure resembling a parking garage tested on the Network for Earthquake Engineering Simulation (NEES) Large High-Performance Outdoor Shake Table at the University of California at San Diego. Detailed information on the test specimen geometry, material tests and loading sequence can be found elsewhere [11, 12].

A picture of the tested structure and wall dimensions are shown in Figure 1, while the relevant data for the finite element analyses are reported in Table 1. The total mass of each floor, taking into account the tributary mass of the columns, is 36795 kg, 38999 kg and 34230 kg for the 1st, 2nd and 3rd floor, respectively; it is worth noting that a vertical slotted connection between the wall and the floors allowed to transfer only horizontal loads.

The walls were designed to act as rocking walls for low intensity tests and as hybrid walls for moderate and high seismic hazard. In the present paper only the rocking wall configuration is considered. The input motion adopted for the selected case study represents a design basis earthquake for Knoxville (TN – USA); the pseudo acceleration spectrum is shown in Figure 2. It is worth noting that similitude law was not achieved by mass substitution but only by scaling the input ground motions, horizontal acceleration field amplified by 1.855 and ground motions time step compressed by 1.855, therefore for sake of clarity the results will be presented herein in dimensionless terms.

Figure 1: Tested structure and wall dimensions.

Unconfined concrete properties [16]	
Strength (f'_c) average of two cylinder tests	54 MPa
Elastic modulus (E_c)	37000 MPa
Strain at maximum stress (ε_{c0})	0.2%
Ultimate compressive strain	0.55%
Confined concrete properties [16]	
Confined maximum stress (f'_{cc})	80.8 MPa
Strain at maximum stress (ε_{cc})	0.67%
Ultimate compressive strain (ε_{cu})	3.77%
Unbonded prestress tendons	
Tendon set	5 x 0.5" strands
Prestressing force for each tendon set	235.75 kN
Unbonded length	8529 mm

Table 1: Rocking wall relevant properties.

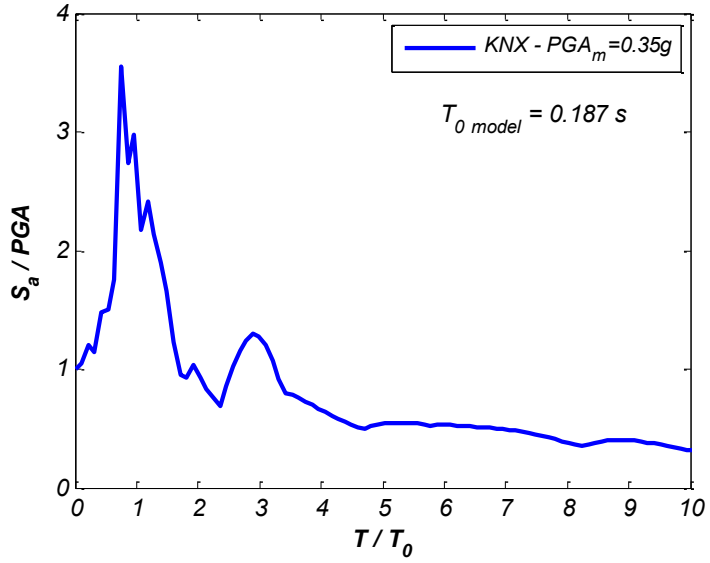

Figure 2: Pseudo acceleration spectrum (ξ = 0.05%).

3 FINITE ELEMENT MODELING

The finite element models presented herein represent a single rocking wall panel (Figure 1), being the scope of the paper the investigation of different modeling techniques with no interest on the global interaction between the wall and the building and the local influence of the foundation beam in the rocking wall response. The foundation is made deliberately rigid by increasing the concrete elastic modulus by two orders of magnitude for the 3D and 2D elements representation and it is modeled consistently in all the 1D elements models in order to achieve the same rotational stiffness. The tributary mass of each floor is modeled as lumped horizontal mass at the wall center line corresponding to the floor height. The wall mass is considered directly starting from the wall material density.

Mander model [16] is adopted to describe the material stress-strain relationship for confined and unconfined concrete, while the formulation contained in the PCI Handbook [17] is considered for the prestressing strands.

3.1 3D and 2D elements models

The 3D and 2D elements models analyses are performed with the finite element software Abaqus [18] adopting brick elements (3D elements model) and plane stress elements (2D elements model) for the wall panel and the foundation and truss elements for the prestressing tendons. The inelastic properties of the concrete are taken into account with the "concrete damaged plasticity model" available in the software package, a viscosity parameter of 0.0004 is added for convergence issues; the tendons inelastic component is modeled with a plastic isotropic material model.

The foundation, whose arbitrary chosen dimensions are 3000x500x203mm, is made to act as a rigid body increasing the concrete elastic modulus by two orders of magnitude. The connection between the wall and the foundation is modeled using a "surface to surface contact" interaction, with tangential behavior type "rough" and normal behavior type "hard contact" under compressive stress: this model allows vertical uplift and avoid horizontal slippage.

The unbounded tendons are modeled as truss elements pinned connected to the ground at the base and rigidly connected to the top of the wall by means of the "beam" type multi point constrain [18]. The vertical and horizontal reinforcing steel bars of the wall confined toe region are modeled as one-dimensional beam elements directly embedded in the concrete matrix only for the 2D elements model.

Three loading steps are created: in the first load step the boundary conditions are set and the gravity load is applied to the model; in the second load step prestressing force is applied to each tendon; in the third load step the nonlinear static or dynamic analysis is performed.

A mesh composed of quad-dominated elements with 4-node bilinear plane stress elements and reduced integration is used both for the wall and the foundation in the 2D elements model while 8-node linear bricks with reduced integration are adopted in the 3D elements model (Figure 3). The foundation element size is 100mm while the wall element size varies from 200mm, at the top of the wall, to 25mm, at the toe regions, for a better description of local effects during base joint opening. Higher order elements and a refined discretization led to similar output results and are not presented herein.

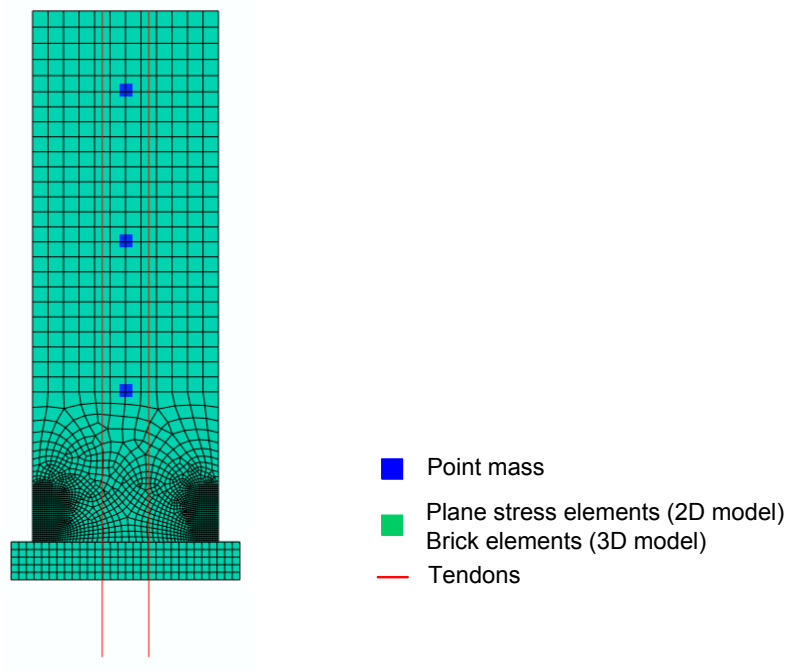

Figure 3: Representation of the 2D/3D elements models.

In the nonlinear dynamic analyses, no global damping is assigned to the model; mass proportional material damping (β=0.00623) is provided only in the wall for convergence issues.

3.2 1D elements models

Three 1D element models are considered in the paper adopting basic and advanced features of the finite element software MidasGEN [20]: fiber elements (*Fb*) model, multi-springs (*MS*) model and rotational spring (*RS*) model (Figure 4).

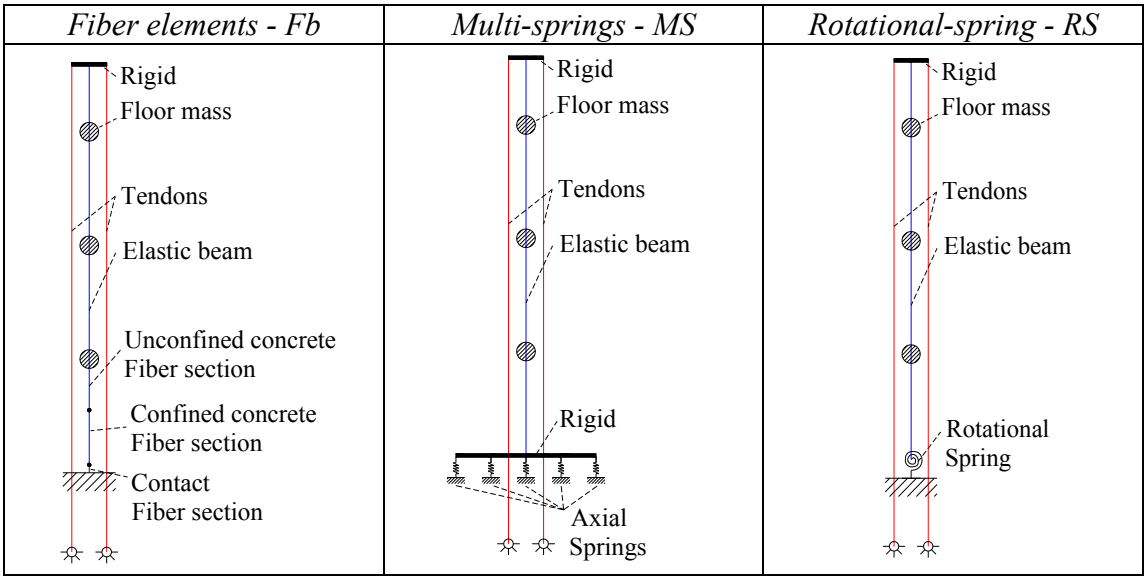

Figure 4: Representation of the 1D elements models.

In the *Fb* model (Figure 4), different fiber sections are used in order to describe the behavior of the wall and wall-foundation interaction. Regular fiber sections are adopted in the wall panel considering nonlinear stress-strain relationship for the confined and unconfined concrete and the reinforcing bars. No fiber elements are placed above the first floor being the response in that region essentially elastic. To simulate the wall-foundation interaction, a fiber section with no reinforcing bars and with no tensile strength concrete is positioned between the wall base and the ground with a stress-strain relationship consistent with the 2D elements model foundation.

The fiber elements adopted in the analyses are based on a force formulation and on the assumption of plane sections remaining plane during the analysis. This is in contrast with the actual strain distribution in the rocking wall discontinuity region which extends from the wall-foundation interface up to approximately a height equal to the wall width. Following the element formulation assumptions, the first section at the base of the wall will exhibit reinforcing bars in tension also during uplift of the wall base which clearly violates the equilibrium of the real situation. Therefore this formulation is suitable to describe rocking walls in global terms, base shear – base rotation relationship, but inappropriate for the local behavior at the wall base, contact length and strain distribution.

Prestressing tendons modeling is the same for all the three 1D elements models. Each tendon set is constituted by a truss element pinned connected at the base and rigidly connected at the top to the wall by means of a stiff beam element. The possible contact between each tendon and the relative duct during wall rotation is not considered. The inelastic behavior, in terms of force-displacement relationship, is taken into account with a normal bilinear lumped plasticity hinge.

In the *MS* model (Figure 4) the support of the wall on the foundation is schematized with a series of axial springs acting only in compression to allow separation between the wall and the foundation during rocking. The elastic stiffness of each spring is EA/H where, according to the 2D elements model foundation, E and H are respectively the elastic modulus and the height of the foundation and A is the influence area of each spring. As it will be shown in the next section, the aforementioned axial spring stiffness leads to stiffer results in the initial part of the shear-rotation relationship compared to 2D elements models. Therefore another tentative axial stiffness formulation is adopted considering the resultant stiffness of two springs in series: the first spring is the aforementioned spring simulating the foundation and the second spring takes into account somehow the wall flexibility in the contact region. To accomplish this, the latter spring stiffness is evaluated as EA/(0.15 l_w) where E is the elastic modulus of the wall concrete, A is the influence area of each spring and 0.15 l_w, being l_w the wall length, represents the wall base neutral axis value at stiffness change in the shear-rotation relationship, therefore considering the axial stiffness of a portion of the wall base with height equal to the neutral axis depth. Yielding of concrete in compression is also introduced in each axial spring with a normal bilinear model. The influence of the number of springs is also investigated taking into account four different models with 99, 25 and 15 springs respectively.

In the *RS* model (Figure 4), the simplest model presented in this paper, the wall panel is modeled with an elastic beam pin-connected to the ground, the interaction between the wall and the foundation is described by means of a nonlinear rotational spring connecting the wall base to the ground. The difficulty of this model arises from the definition of appropriate nonlinear properties of the rotational spring. A possible solution is the adoption of elastic bilinear or multilinear analytical formulations available in the literature such as the one proposed by Restrepo and Rahman [6]. For sake of clarity between the 1D elements models comparison, in the present paper the rotational spring is calibrated according to the 2D elements model adopting an elastic trilinear representation.

In all the models, especially in the simplified 1D elements models, special care must be placed in the choice of numerical damping [20-22], adopted in the dynamic analyses to take into account all the sources and mechanisms of energy dissipation not directly considered in the material hysteretic behavior. The most common and well known representation of damping is Rayleigh damping, in which the viscous damping matrix is obtained as a linear combination of the mass and stiffness matrixes:

$$\boldsymbol{C} = \alpha \boldsymbol{K} + \beta \boldsymbol{M} \tag{1}$$

In the case of rocking walls, such a formulation could lead to fictitious viscous forces at the base of the wall, especially if initial stiffness matrix is considered in the damping formulation. In fact, during rocking of the wall the base gap opens and the wall and foundation points, *Fb* and *MS* models, gain relative velocity and therefore viscous forces arises in those positions if the initial elastic stiffness is considered in damping formulation. Analogous considerations apply in the case of *RS* model, where the initial elastic rotational stiffness is significantly higher than the stiffness associated to the gap opening: when the base rotational spring reaches the yield point, it gains rotational velocity and therefore a viscous moment arises.

This fictitious forces and moments introduce unrealistic sources of resistance and viscous energy dissipation at the base of the wall and lead to a significant underestimation of the structural seismic demand. To avoid this problem tangent stiffness proportional damping must be adopted.

In the 1D element models presented in the paper, only the results of tangent stiffness proportional damping are considered, both in the case of Rayleigh damping and stiffness proportional damping. The stiffness proportional coefficient α (Eqn.1) is obtained assigning the

selected relative damping ratio to the structural first mode period. In the case of Rayleigh damping the coefficients α and β (Eqn.1) are obtained assigning the selected relative damping ratio to the structural first mode period and to the period corresponding to the shear-rotation post yield stiffness, which corresponds in the present case to 10 times the fundamental period.

4 FINITE ELEMENT ANALYSES RESULTS

In this section the results of the nonlinear static and dynamic analyses are presented. For sake of clarity, being the rocking wall representative of a scaled structure, the results are presented in dimensionless terms: the neutral axis depth is normalized to the wall length, the base shear to the model weight (621.3 kN) corresponding to half of the total weight of the tested structure, and the accelerations to the PGA (0.35g).

4.1 Nonlinear Static Analyses Results

The nonlinear static results of the 2D and 3D elements models are shown in global and local terms in Figure 5 and Figure 6 respectively. The 2D and 3D elements models considering the concrete as a linear elastic material show basically the same behavior both in global and local terms. When nonlinear concrete behavior is introduced in the wall there is, as expected, an increase in the axial compressive strains. This increase is higher in the 2D than in the 3D elements model, although these results sould be compared with actual values obtained from experimental tests to check finite element model suitability.

The implementation of the longitudinal and transverse rebars in the confined area at the base of the wall reduced both neutral axis and strain values compared to the case in which only concrete nonlinearity is considered.

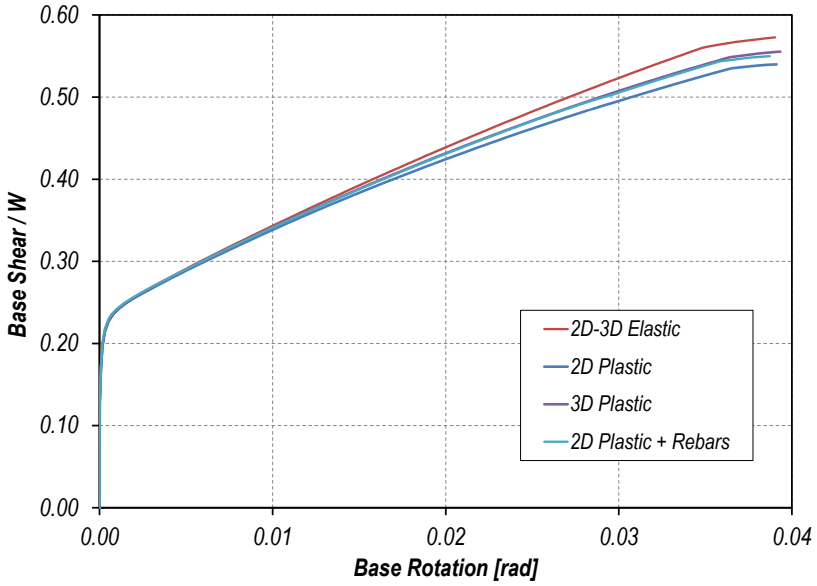

Figure 5: Base shear – base rotation 2D-3D elements models.

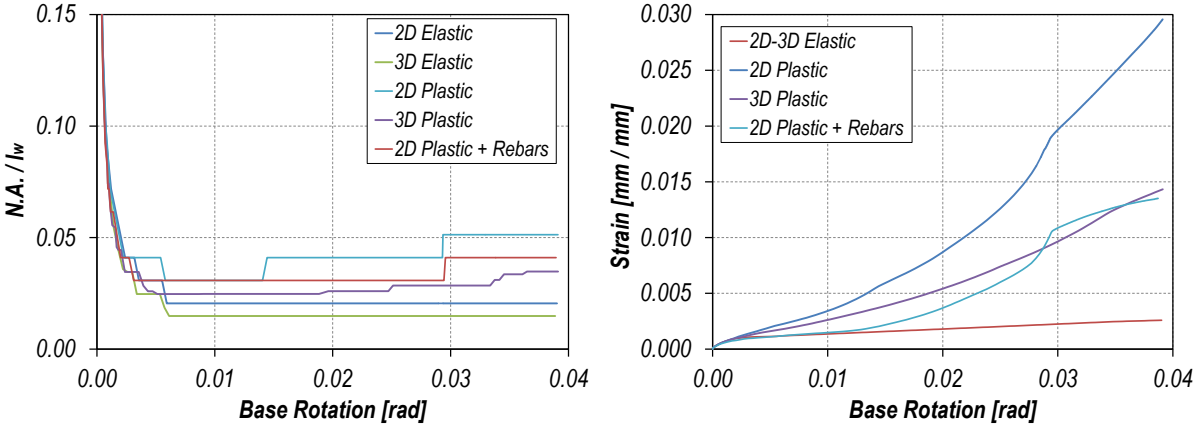

Figure 6: Neutral axis variation and concrete compressive strain 2D-3D elements models.

Regarding 1D elements models, Figure 7 shows the influence of the number of axial compression only springs in *MS* model on the base shear – base rotation response. There is basically no difference between 99 and 25 axial springs models while there is an increase in the post yield stiffness in the case of 15 springs, which is associated to the concentration of the compressive force in the last external spring. It is therefore suggested to have at least 2 springs fully in contact in the minimum expected neutral axis depth. Figure 7 shows also the stiffer response at the apparent yield point in the case of axial springs with stiffness equal to the solely foundation stiffness (*"MS_f – 99 Springs"* model).

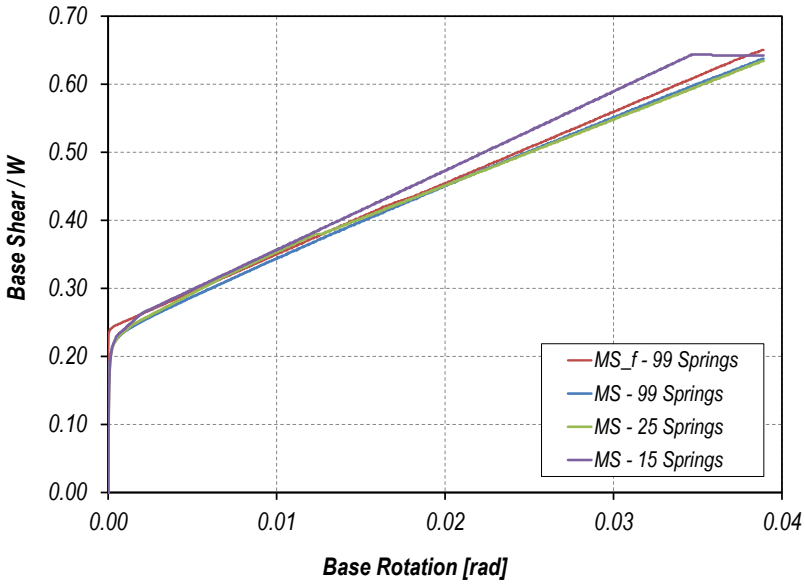

Figure 7: Base shear – base rotation MS models as a function of axial springs number.

Figure 8 compares the base shear – base rotation response of all the 1D elements models and the 2D elements model plus rebars in the confined region. The same figure contains the bilinear elastic response proposed by Restrepo and Rahman [6]. *Fb* model and Restrepo and Rahman bilinear approximation show a stiffer response in the post yield region. *Fb* and *RS* models also present an abrupt change in the apparent yield region which causes high horizontal spikes in the dynamic response as it will be shown later. Among the 1D elements models, *MS* model gives the best global response approximation.

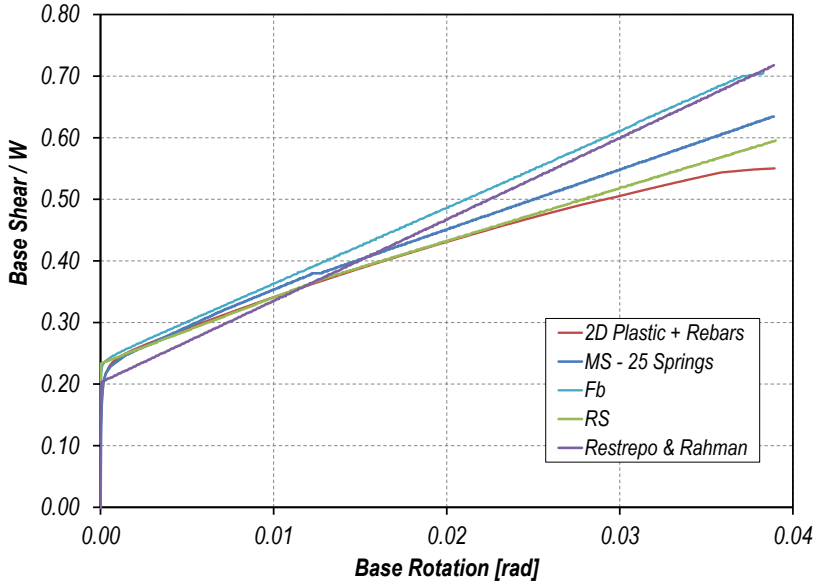

Figure 8: Base shear – base rotation 1D elements models.

Figure 9 shows the 1D elements response in local terms. Only *Fb* and *MS* models allow to determine the neutral axis variation and only *Fb* model provides concrete strains, although their values are not reliable as evident in the figure and explained before.

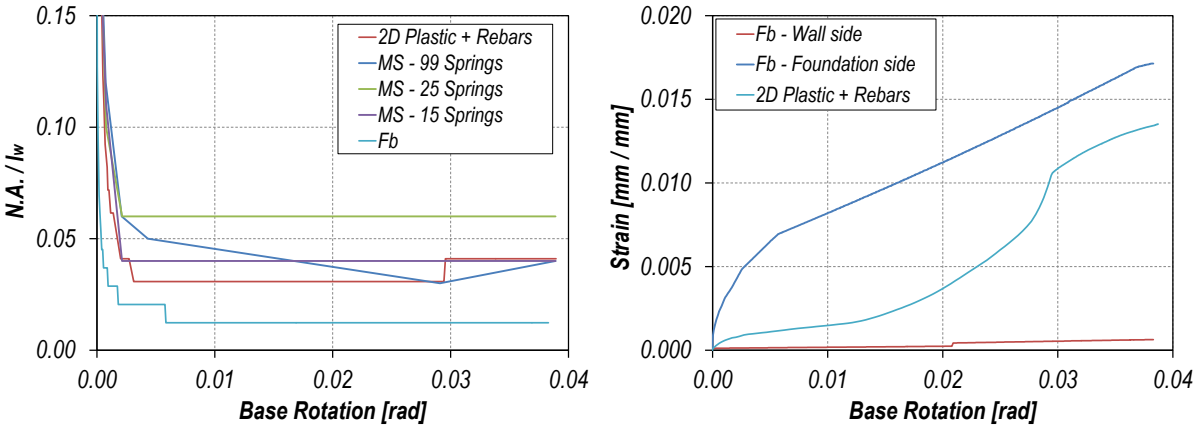

Figure 9: Neutral axis variation and concrete compressive strain 1D elements models.

Even though not presented in graphical format, another feature worth of being investigated is the vertical uplift at the wall center line which influences geometric compatibility and interaction between the wall and adjacent elements. Among the 1D elements models only the *RS* one is not able to capture the wall vertical uplift, in fact in this model wall uplift is not provided at all.

4.2 Nonlinear Time History Analyses Results

This section presents the results of nonlinear dynamic analyses. Being the seismic demand limited according to the low seismicity site chosen (Knoxville-TN), the expected base gap opening is limited to few milliradians. For these rotation values the local and global behavior of the different 2D and 3D elements models investigated is very close, therefore only the re-

sults of the 2D elements with rebars in the confined region are presented as representative of 2D and 3D elements models.

Figure 10 shows the base shear - base rotation response of the 2D elements model and the experimental test results, being the latter added only for qualitative comparison as the present paper does not intend to capture the dynamic interactions between the walls and the floors and the influence of the foundation. From the graph it is possible to see how the 2D elements model is able to describe the global rocking wall behavior and to capture base shear peaks for wall base rotations close to zero. These peaks are associated to horizontal acceleration spikes (Figure 11) arising when the wall gains horizontal lateral stiffness in the unloading phase, as explained and showed elsewhere [12, 23], which happens in proximity of zero base rotation. Figure 11 shows horizontal (a_h) and vertical (a_v, positive upward, acceleration of gravity excluded) acceleration time histories at the wall 3rd floor.

The peaks in vertical acceleration arise when the wall base gap closes [12] and show higher values compared to experimental test due to the increased stiffness of the foundation beam model compared to the actual tested structure.

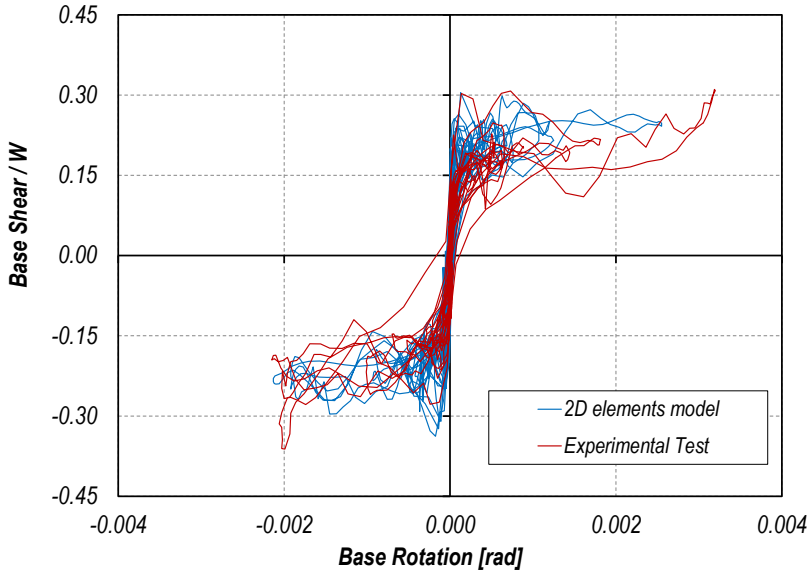

Figure 10: Base shear – base rotation for the 2D elements model and the tested structure.

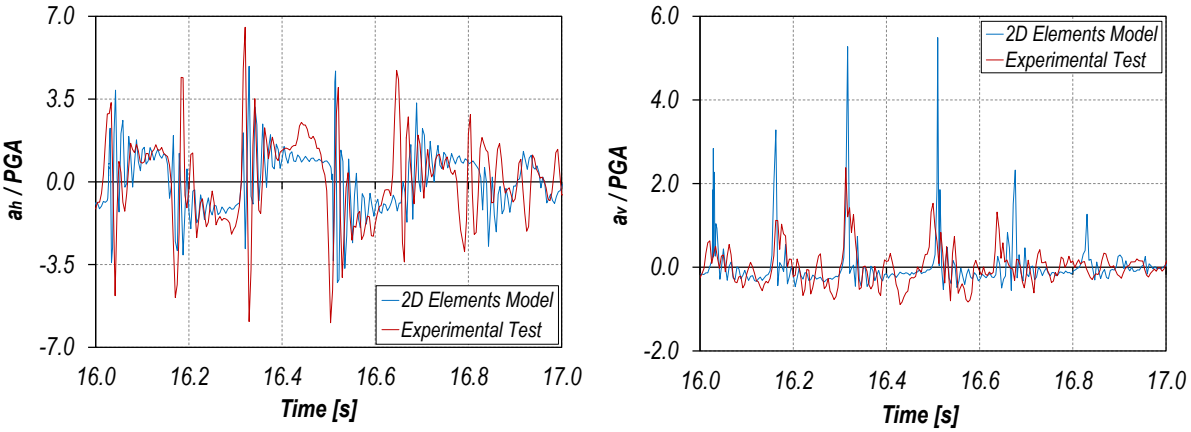

Figure 11: Horizontal (a_h) and vertical (a_v) acceleration for the 2D elements model and the tested structure.

Regarding 1D elements models, the comparison is made between two damping formulations, Rayleigh (R) damping and stiffness proportional (SP) damping, both considering tangent stiffness proportionality at each time increment in the damping matrix definition. A damping ratio of 3% is selected for each formulation in the way explained before.

Figure 12, Figure 13 and Figure 14 show, respectively, the base shear - base rotation, horizontal acceleration and vertical acceleration of the 1D elements models and the comparison with the 2D element model response.

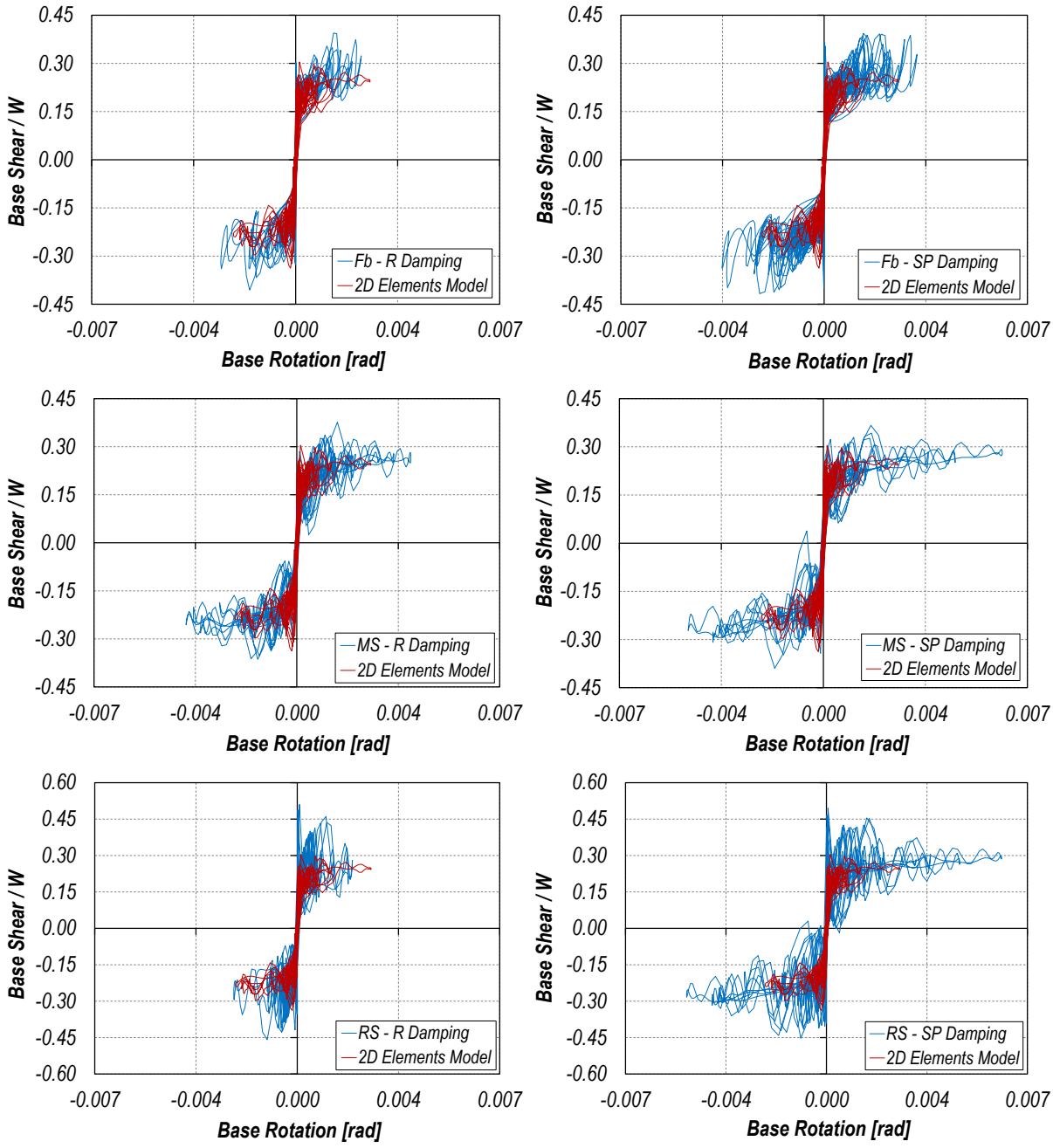

Figure 12: Base shear – base rotation 1D elements models; comparison with 2D elements model.
Note: Fb = Fiber elements; MS = Multi-Spring; RS = Rotational Spring;
R damping = Rayleigh damping; SP damping = Stiffness Proportional damping.

The results indicate how 1D elements models could significantly over-predict the structural response, both in base shear and base rotation terms, depending on the damping formulation chosen and on the selected damping ratio.

Horizontal acceleration significantly differs between the 2D elements model and the *Fb* and *MS* models. In the *RS* model horizontal acceleration spikes are qualitatively similar to 2D elements model, although, as stated before, base shear values are over-predicted.

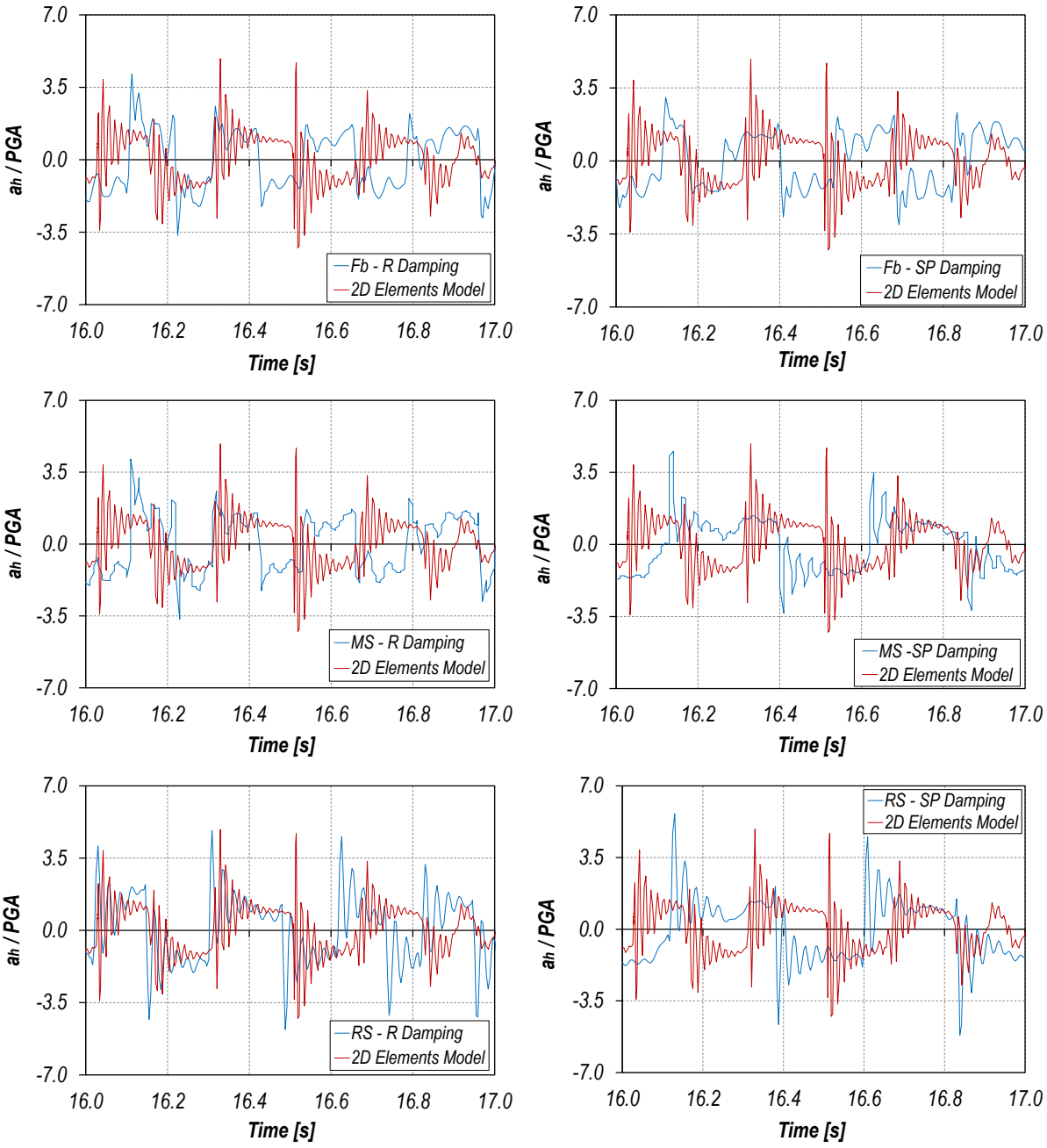

Figure 13: Horizontal acceleration 1D elements models; comparison with 2D elements model.
Note: Fb = Fiber elements; MS = Multi-Spring; RS = Rotational Spring;
R damping = Rayleigh damping; SP damping = Stiffness Proportional damping.

Vertical acceleration spikes are better captured by the *MS* model; *RS* model does not consider wall uplift and therefore the vertical acceleration (a_v) in this model is zero.

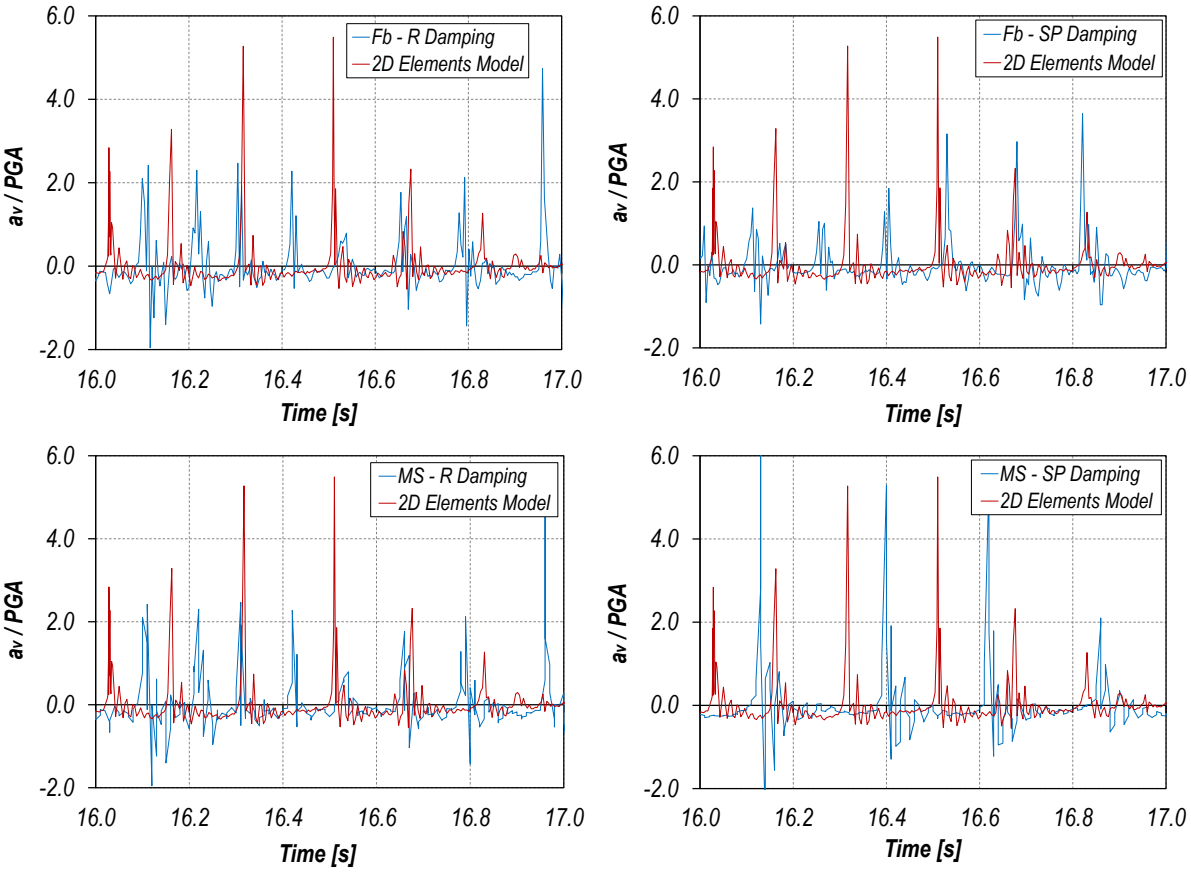

Figure 14: Vertical acceleration 1D elements models; comparison with 2D elements model.
Note: Fb = Fiber elements; MS = Multi-Spring;
R damping = Rayleigh damping; SP damping = Stiffness Proportional damping.

Figure 15 shows the results of 1D elements models after tuning the damping ratio value, in tangent stiffness proportional formulation, in order to obtain approximately the same maximum base rotation of the 2D elements model. The damping ratios chosen are 0.061, 0.144 and 0.142 for the *Fb*, *MS* and *RS* models respectively.

The results show how with the selected damping values the 1D elements models predict quite well the rocking wall behavior in global terms, although significant differences are present close to zero base rotation being the horizontal acceleration spikes, arising when the wall approaches the rest position, damped out. This could underestimate the base shear demand in those regions and causing wall horizontal slippage if relying solely on friction in the base shear transfer mechanism [12].

The vertical acceleration spikes are only slightly affected by the selected damping ratios.

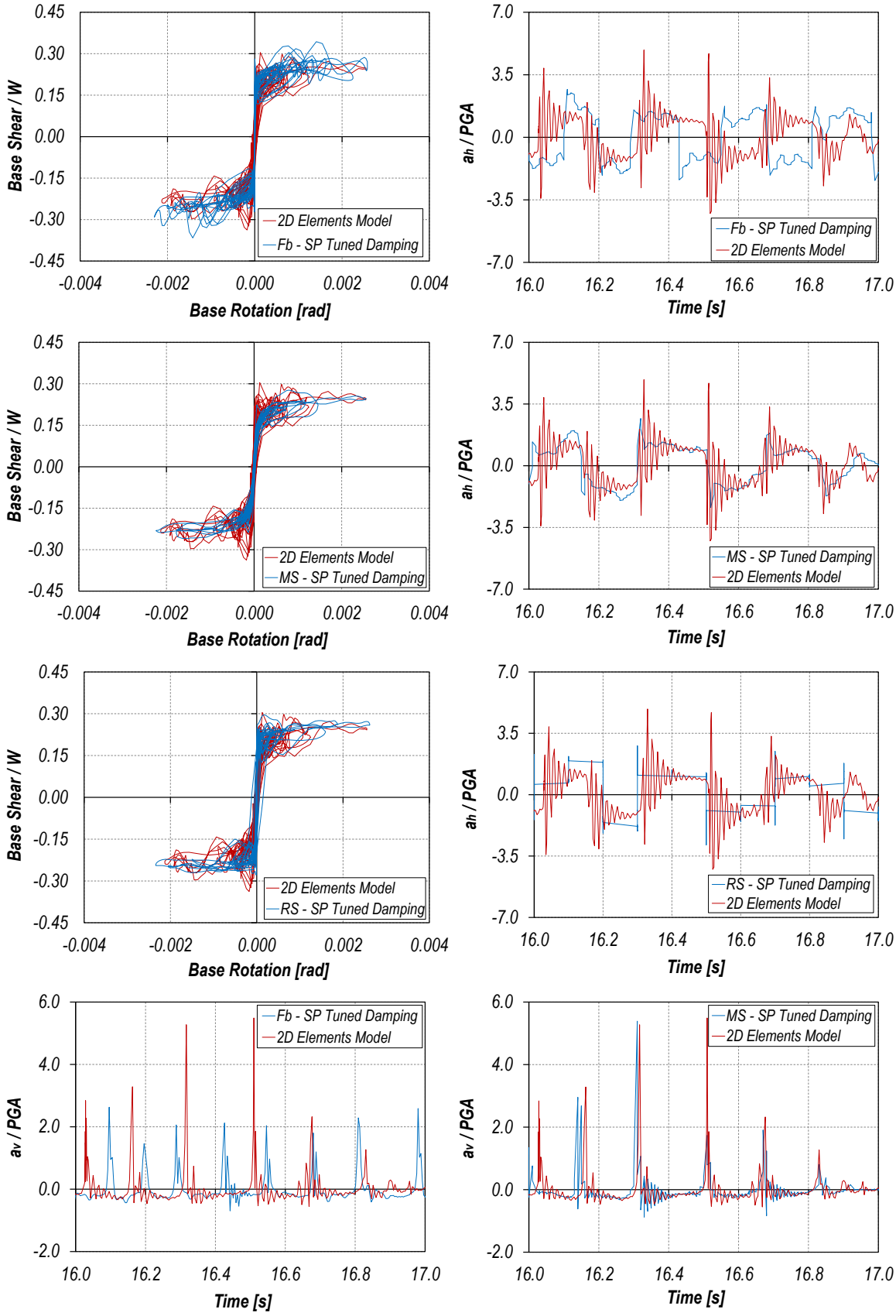

Figure 15: Base shear – base rotation, horizontal and vertical acceleration
1D elements models with tuned damping.

5 CONCLUSIONS

In the present paper the finite element modeling of rocking walls is considered in order to highlight differences between different modeling techniques comprising 3D, 2D and 1D elements. The dynamic interaction between the wall and the building and the influence of the foundation is beyond the purpose of the paper and therefore neglected in the investigation.

The results of the research show that 3D and 2D models are the only suitable to describe the rocking wall behavior in local terms, neutral axis variation and wall toe concrete compressive strains. 3D elements models considering concrete nonlinearities provide lower concrete compressive strains compared to the corresponding 2D elements models. To determine the most reliable model in terms of strain prediction, comparisons to test results are needed.

The 1D elements models considered are based on fiber elements (*Fb*), multi compression only springs (*MS*) and concentrated rotational spring (*RS*). These models allow to capture the rocking wall behavior in global terms, base shear - base rotation relationship, although differences arise in the nonlinear static analyses compared to 2D elements model results. *Fb* model and Restrepo and Rahman [6] bilinear approximation, commonly adopted in the *RS* model definition, show a stiffer response in the post yield region. *Fb* and *RS* models also present an abrupt change in the apparent yield region. Among the 1D elements models, *MS* model gives the best global response approximation in nonlinear static analyses. It is worth to note that *RS* model does not allow wall center line uplift and therefore with this model it is not possible to capture interactions between the wall and adjacent elements.

Regarding nonlinear dynamic analyses, 2D and 3D models provide results qualitatively similar to the experimental test without the addition of global damping. In the case of 1D elements models global damping was needed for convergence issues and the results are strongly influenced by the chosen damping formulation. The use of Rayleigh or stiffness proportional damping without damping matrix update, that is proportional to initial elastic stiffness, leads to unconservative results and therefore should be avoided; this is associated to the development of fictitious viscous forces (*Fb* and *MS* models), or moments (*RS* model), at the base of the wall which unrealistically increase the wall base capacity and viscous energy dissipation. Better results are obtained when damping matrix is formulated proportionally to tangent stiffness, both in the case of Rayleigh and stiffness proportional damping.

Tangent stiffness proportional damping formulation overestimates the wall response in terms of base shear and base rotation compared to Rayleigh damping. This could be overcome by increasing the damping in the former formulation although in this way there is a significant under-prediction of the horizontal acceleration spikes especially around zero base rotation. Among 1D elements models, *Fb* model gives closer results to 2D elements model with lower damping ratios compared to *MS* and *RS* models.

ACKNOWLEDGEMENTS

The authors wish to express their gratitude to the Precast/Prestressed Concrete Institute, the National Science Foundation, the Charles Pankow Foundation, and the George E. Brown Jr. Network for Earthquake Engineering Simulation and all the people involved in the DSDM project especially to Prof. R.B. Fleischman at the UA, prof. J.I. Restrepo at the UCSD and to Dr. M.J. Schoettler at the UC Berkeley. The opinions, findings, and conclusions expressed in the paper are those of the authors and do not necessarily reflect the views of the individuals and organizations involved in the DSDM project.

REFERENCES

[1] Y. Osanai, F. Watanabe, S. Okamoto, Stress Transfer Mechanism of Socket Base Connections with Precast Concrete Columns, *ACI Structural Journal*, **93**: 3, 1-11, 1996

[2] J. J. Blandón, M. E. Rodríguez, Behavior of Connections and Floor Diaphragms in Seismic- Resisting Precast Concrete Buildings, *PCI Journal*, **50**:2, 56-75, 2005.

[3] A. Belleri, P. Riva, Seismic performance and retrofit of precast grouted sleeve connections, *PCI Journal*, **57**:1, 97-109, 2012.

[4] J. I. Restrepo, R. Park, A. H. Buchanan, Design of Connections of Earthquake Resisting Precast Reinforced Concrete Perimeter Frames, *PCI Journal*, **40**:5, 68-80, 1995.

[5] M. J. N. Priestley, S. Sritharan, J. R. Conley, S. Pampanin, Preliminary Results and Conclusions from the PRESSS Five-Story Precast Concrete Test-Building, *PCI Journal*, **44**:6, 42-67, 1999.

[6] J. I. Restrepo, A. Rahman, Seismic Performance of Self-Centering Structural Walls Incorporating Energy Dissipators, *Journal of Structural Engineering*, **133**:11, 1560-1570, 2007.

[7] F. J. Pérez, R. Sause, S. Pessiki, Analytical and experimental lateral load behavior of unbonded posttensioned precast concrete walls, *Journal of Structural Engineering*, **133**:11, 1531-1540, 2007.

[8] Y. C. Kurama, Hybrid Post-Tensioned Precast Concrete Walls for Use in Seismic Regions, *PCI Journal*, **47**:5, 36-59, 2002.

[9] D. Marriott, S. Pampanin, D. Bull, A. Palermo, Dynamic Testing of Precast Post- Tensioned Rocking Walls Systems with Alternative Dissipating Solutions, *Bulletin of the New Zealand Society for Earthquake Engineering*, **41**:2, 90-103, 2008.

[10] R. B. Fleischman, C. Naito, J. Restrepo, R. Sause, S. K. Ghosh, G. Wan, M. Schoettler, L. Cao, Precast Diaphragm Seismic Design Methodology (DSDM) Project, Part 2: Research Program, *PCI Journal*, **50**:6, 14-31, 2005.

[11] M. J. Schoettler, A. Belleri, D. Zhang, J. I. Restrepo, R. B. Fleischman, Preliminary results of the shake-table testing for the development of a diaphragm seismic design methodology. *PCI Journal*; 2009; **54**(1), 100-124, 2009.

[12] A. Belleri, M. J. Schoettler, J. I. Restrepo, R. B. Fleischman, Dynamic behavior of rocking and hybrid cantilever walls in a precast concrete building. Accepted at *ACI Structural Journal*, 06/02/2013.

[13] Y. C. Kurama, R. Sause, S. Pessiki, L. Le-Wu, Lateral Load Behavior and Seismic Design of Unbonded Post-Tensioned Precast Concrete Walls. *ACI Structural Journal*, **96**:4, 622-632, 1999.

[14] B. Erkmen, A. E. Schultz, Self-Centering Behavior of Unbonded, Post-Tensioned Precast Concrete Shear Walls. *Journal of Earthquake Engineering*, **13**, 1047-1064, 2009.

[15] W. Y. Kam, S. Pampanin, A. Palermo, A. J. Carr, Self-centering structural systems with combination of hysteretic and viscous energy dissipations. *Earthquake Engineering and Structural Dynamics*, **39**, 1083-1108, 2010.

[16] J. B. Mander, M. J. N. Priestley, R. Park, Theoretical stress-strain model for confined concrete, *Journal of Structural Engineering,* **114**:8, 1804-1826, 1988.

[17] PCI Industry Handbook Committee, PCI Design Handbook: Precast and Prestressed Concrete. 6th ed. Chicago-IL, 2004.

[18] ABAQUS user's manual version 6.11. Dassault Systèmes Simulia Corp., 2011.

[19] MidasGEN 2012 (v3.1), MIDAS Information Technologies Co. Ltd.

[20] F. A. Charney, Unintended consequences of Modeling Damping in Structures, *ASCE Journal of Structural Engineering*, **134**:4, 581-592, 2008.

[21] J. F. Hall, Problems encountered from the use (or misuse) of Rayleigh damping, *Earthquake Engineering and Structural Dynamics*, 35, 525-545, 2006.

[22] L. Petrini, C. Maggi, M. J. Priestley, G. M. Calvi, Experimental Verification of Viscous Damping Modeling for Inlelastic Time History Analyzes, *Journal of Earthquake Engineering*, **12(S1)**, 125-145, 2008.

[23] L. Wiebe, C. Christopoulos, Characterizing acceleration spikes due to stiffness changes in nonlinear systems, *Earthquake Engineering and Structural Dynamics*, **39**, 2010, 1653-1670, 2010.